MUSIC Speciation of γ-Al 2 O 3 at the Solid Liquid Interface: How DFT Calculations Can Help with Amorphous and Poorly Crystalline Materials

Manuel Corral Valero, Bénédicte Prélot, Grégory Lefèvre

MUSIC Speciation of γ-Al_2O_3 at the Solid Liquid Interface: How DFT Calculations can Help with Amorphous and Poorly Crystalline Materials

Manuel Corral Valero[1], Bénédicte Prelot[2], Grégory Lefèvre[3,*]

[1]IFP Energies nouvelles, Direction Catalyse et Séparation, Rond-point de l'échangeur de Solaize, 69360 Solaize (France)

[2] Institut Charles Gerhardt, UMR-5253 CNRS-UM-ENSCM, Université de Montpellier, Place E. Bataillon, F-34095 Montpellier cedex 5, France

[3] Chimie ParisTech, PSL Research University, CNRS, Institut de Recherche de Chimie Paris (IRCP), F-75005 Paris, France

* Corresponding author. E-mail address: Gregory.Lefevre@chimie-paristech.fr

ABSTRACT

Transition aluminum oxides, such as γ-Al_2O_3 or alumina, are widely used in many different technical applications that rely on the surface reactivity of this material at the solid liquid interface. The speciation of surface sites of this material confronts several obstacles. On the one hand, alumina is a poorly crystalline oxide, thus allowing for a limited amount of empirical structural information for an important number of surface sites with different trends in reactivity and, on the other hand, it is a metastable material. In this work, we show several ways in which the Multi Site Complexation Model (MUSIC), combined with atomistic information from Density Functional Theory and Ab Initio Molecular Dynamics, can manage to perform speciation calculations of γ-Al_2O_3 surface sites at the solid liquid interface. Although the results are in good qualitative agreement with experimental titration curves, and they can serve as a guide for the interpretation of the reactivity of this material at the initial stages of an impregnation experiment and chemical weathering phenomena, this work highlights the need of more complex AIMD simulations to accurately model these phenomena in γ-Al_2O_3 surface/liquid interfaces.

KEYWORDS: Multisite complexation (MUSIC); Density Functional Theory (DFT); alumina; surface speciation; surface reactivity; Solid Liquid Interface; Ab Initio Molecular Dynamics (AIMD)

1. INTRODUCTION

Among the different transition aluminum oxides, γ-Al_2O_3 –also referred to as alumina- is one of the most widespread materials in a variety of technical applications and, in particular, for heterogeneous catalysis supports[1] and water treatment [2]. Hence, predicting the retention of metals and organic species by this compound at the solid liquid interface (SLI) is of paramount importance. Unfortunately, γ-Al_2O_3 is also poorly cristallineand extremely difficult to characterize rigorously by most conventional analytical techniques. However, complex Density Functional Theory (DFT) calculations has been successfully performed to obtain a detailed atomic description of physicochemical phenomena (see Raybaud *et al.* [3,4] for a review). Moreover, this is a metastable material and its bulk structure changes in presence of water [5,6]; this process takes some time to be detected and the rate and extent to which surface groups are affected by this evolution is not fully understood. Besides, there is evidence that this process may be inhibited by the sorption of inorganic species [7].

Despite these difficulties, there have been attempts to depict the structure and reactivity of γ-Al_2O_3 surfaces at the SLI [8–10] from DFT based Ab Initio Molecular Dynamics (AIMD) simulations. These theoretical results provides insights about the properties of this material in contact with water at short time scales –before the subsequent transformation of alumina by water or its inhibition by the adsorption of a species. Therefore, these studies could provide a starting point for future detailed analysis of the evolution of alumina in contact with water and its inhibition by the adsorption of water at the atomic scale (as in, for example, reference [10]).

When it comes to the reactivity of amorphous or poorly cristalline materials in water, effective 1-pKa and 2-pKa models are used [11,12]. This allows for a rationalization of sorption experiments, although at the cost of a detailed description of phenomena at the atomic scale. In the case of alumina, works from Raybaud *et al.* shows that γ-Al_2O_3 surfaces present about 3 classes of sites with different

reactivity[13,14]. Hence, atomistic models for this material, at the SLI and based on first principles approaches, could be a starting point for rationalizing their reactivity.

The so-called MUSIC model from Hiemstra and co-workers (see [15,16] for the original model and [17,18] for refinements of this work) allows for a prediction of the protonation constant (pKa) of surface OH groups on metal (hydr)oxides based on atomic scale information, mainly the number of bonds around surface species and their effective charge. Thus, MUSIC-based pKa constants in conjunction with an electrical double layer model has been successfully used to simulate the surface charge of complex metal oxides in water [19]. The bottleneck for the application of this approach to an amorphous or poorly crystalline material remains the lack of information about the structural parameters of the involved surfaces sites. In literature, this problem has been resolved by a so-called pragmatic approach, where the authors described the mean surface reactivity with only one surface site ($>SO^{1/2-}$ in its deprotonated state) and one equilibrium reaction ($>SO^{1/2-} + H^{+} = >SOH^{1/2+}$) with a pK equal to the Point of Zero Charge (PZC) [20]. Moreover, Hiemstra et al.[15] have described the surface reactivity with the singly coordinated AlOH found on gibbsite ($pK_{1,2} = 9$), associated to a $>SO^{1/2-}$ with a pK equal to 7 (chosen from the experimental value of the PZC). In the work by Nagashima and Blum [21], authors assumed that only Al^{VI} are present at the surface and fit the acid-base titration curves to obtain the densities of the surface groups. Thus, in these works, even if crystallography-based surface models have been used, the authors have not followed a prediction approach, whose ability is claimed in the MUSIC model, but have rather used them as a starting point of a fitting approach. In this work we propose to use the DFT model of γ-Al_2O_3 surfaces developed by Raybaud *et al.* in [13,14] conjunction with the MUSIC approach for the prediction of alumina's pKa values. To the best of our knowledge, there are few examples in the literature combining DFT and MUSIC calculations and amongst them we may cite those of Kubicki and co-workers [22,23]. In reference [13] DFT calculations were successfully used to depict the reactivity of alumina's surface sites at the solid-gas interface. Moreover, AIMD simulations has been performed in reference [9] in order to obtain a description of this material's structure at the solid water interface. In what follows, we are going to use this

information [9], mainly the coordination number for each OH site, the average number of surrounding hydrogen bonds and an estimate of their surface densities. Protonation constants obtained by these means are used with the Basic Stern double layer model and the speciation software PHREEQC [24] in order to compute the surface charge at the SLI as a function of pH; theoretical results are compared with experimental titration curves.[22] Although results from AIMD simulations in references [8–10] could be considered as a snapshot of γ-Al_2O_3 before the transformations induced by water described [5,6], the results we present here provides insights about the initial stages of this process and opens perspectives for future and more complex works in this area.

2. MATERIALS AND METHODS

The experimental surface charge used for comparison was obtained from titration methods [25]. Measurements were carried out using homemade titration set-up composed of an auto-burette (ABU901) ionometer–pHmeter (PHM250) equipped with GK2401 pH electrode (all from Radiometer), these devices being controlled by the TestPoint procedure. The experimental procedure was adapted from Ali Ahmad et al. [26]. Alumina (0.1 g of γ-Al_2O_3) was first placed in contact with a 50 mL $NaNO_3$ background electrolyte. After acidifications, the suspension was equilibrated during 2 h. The titrations were carried out in the acid-to-base direction by adding a 0.02 mol L^{-1} NaOH titrant. The Background electrolyte was used as reference, with concentration as follows: 10^{-1}, 10^{-2}, and 10^{-3} mol.L^{-1} $NaNO_3$. Experiments were performed in a thermostatic titration cell regulated at 298 K by a thermocryostat and kept under inert gas stream. The surface charge density σ_0 was calculated using the following conventional procedure:

$$\sigma_0 = \frac{-F \cdot C \cdot \Delta V}{m \cdot S} \quad (1)$$

where ΔV is the difference between the volume of titrant added to the suspension (V_s) and that added to the reference phase (V_e) ($\Delta V = V_s - V_e$), F is the Faraday's constant (96500 C.mol^{-1}), C denotes the titrant concentration (mol L^{-1}); m and S refer to the mass (g) and the specific area of the solid

sample ($m^2\ g^{-1}$), respectively. Simulated surface charge for different representations of the particle surfaces have been calculated using the PHREEQC software [24] following the scheme below (Fig. 1).

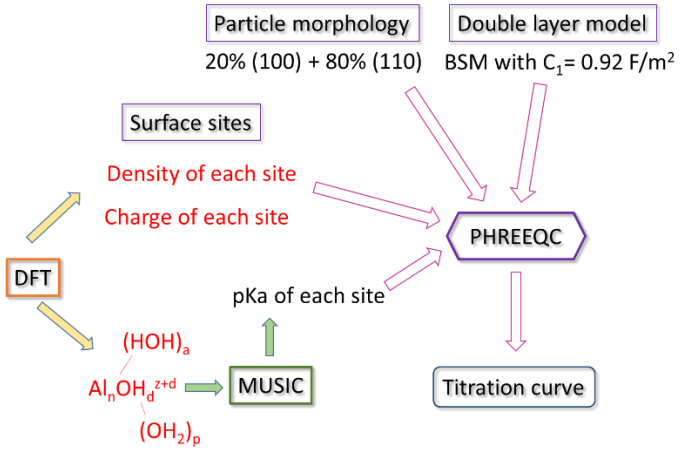

Fig. 1. Scheme of the method followed to simulate the surface charge curves. The inputs coming from DFT calculations are illustrated in red. See text for details.

Several inputs are needed to make this simulation. First, we considered the two most important orientations of alumina's nanocrystallites, the (100) and (110) faces. The atomistic model of these faces is inherited from the bulk model of γ-alumina developed by Krokidis and co-workers in ref. [27] In this work, the authors modeled the topotactic transformation of boehmite (AlOOH) taking place under calcination and leading to γ-alumina. The authors in this paper tested the validity of their model by comparing, on the one hand, experimental and computed XRD patterns and, on the other hand, the Al_{IV}-Al_{VI} distributions in their model with ^{27}Al NMR experiments from previous publications cited therein. The topotactic transformation taking place during boehmite calcination was first reported by Lippens et al. in [28] based on selected area electron diffraction results. In the latter reference, the authors show that exposed faces of boehmite transform in certain faces of γ-alumina. The face indexation in [28] has been used in [13,14] by Digne and co-workers, where the bulk model from reference [27] is used to build the surface models of the hydroxylated (100) and (110) γ-alumina faces at different water coverages (corresponding to different temperature and water partial pressure

exposures); the validity of these surface models was tested by comparing theoretical OH stretch frequencies with experimental FT-IR experiments. In ref. [9] we used the latter results in order to model the reactivity of this material at the SLI. Inspired by the approach of Digne et al., in that paper we also computed the stretching frequencies of alumina's OH groups in presence of water from the velocity autocorrelation function obtained from AIMD simulations.

Both the (100) and (110) orientations account for more than 90 % of the specific surface area and, following the approach in [13] to describe the reactivity at the solid-gas interface, we considered that each accounts for 20 % and 80 % of the specific area, respectively. Second, we used the detailed structural information of surface groups from DFT calculations in ref. [9]. Here, we briefly summarize the methods used in that work. The average structure of the alumina/water interface was obtained from periodic AIMD simulations in the microcanonical ensemble and a time step of 0.5 fs; kinetic energies were rescaled to obtain average temperatures close to 300 K. These simulations were performed within the framework of the Born-Oppenheimer approximation with the CP2K/Quickstep package based on a hybrid Gaussiand and Plane Wave method described in [29], the PBE DFT functional [30,31] with Grimme D2 method for dispersion forces[32], Goedecker-Teter-Hutter pseudopotentials [33] and double-ζ plus polarization Gaussian basis sets for all elements. For the plane waves region, an energy cutoff of 400 Ry was used. Considering the results in [9] (in which different approaches to model the SLI interface for thoses system are compared), we chose to use larger simulation boxes – (2x3) and (2x2) 4-slab thick supercells containing 1164 (96 Al_2O_3 units, 48 adsorbed water molecules and 180 water molecules in the liquid phase) and 1004 (64 Al_2O_3 units, 48 adsorbed water molecules and 180 water molecules) atoms for the (100) and (110) facets, respectively – and shorter simulation times (10 ps after equilibration) in order to obtain structural statistics about the structure of the different surface OH groups (See table 1 for a full account of the different OH groups densities and unit cell vectors in the primitive cell). As for the amount of interfacial water (180 molecules in each cell) it was chosen and kept constant to achieve a density of 1g/L. These water molecules were spread in a volume of 20 Å thickness times the surface area (similar for both cells). It is worth

pointing out that our approach gave results in good agreement with ref. [8] in which a similar analysis was performed about the structure of water at the alumina/water interface.

There is a large variety of hydroxyl groups present in these surfaces; each one is characterized by the coordination of Al atoms (they can be either four coordinated or six coordinated in tetrahedral or octahedral environments, respectively) and the number of Al-O bonds, giving rise to μ_1, μ_2 and μ_3 groups. The full list is presented in Table 1 and Fig. 2. The charge z of each Al_nOH_d group (short name for a real structure shown in Fig. 1) is calculated from the number and the type of Al atom around the oxygen (+0.5 for Al^{VI} or +0.75 for Al^{IV} following the bond valence approach [13,14]), and the number of protons (+1 for each proton). The computation of their pKa values using the MUSIC model is based on the empirical formula given in [18] and retranscripted below in equation 1. Thus, it was found that the protonation constant of a surface site is proportional to the undersaturation of the oxygen valence (the oxygen charge, -2, is not fully neutralized by the electron transfer to the neighbor atoms) and is defined as:

$$\text{Log } K = -19.8\ (\Sigma\ s_{Al} + d.s_H + a.(1- s_H) - 2) \quad (1)$$

Where s_{Al} is +0.5 or +0.75 for VI and IV coordinated Al atoms, respectively, *d* is the number of protons (0, 1 or 2), s_H is +0.8, *a* is the number of accepting hydrogen bonds with water molecule (see Fig. 1); a and d depends on the geometric constraints around the oxygen atom. In the original work, it is assumed that a+d = 2 for simply coordinated groups (μ_1-OH), 1 for triply coordinated groups (μ_3-OH), and 1 or 2 for doubly coordinated groups (μ_2-OH), and that each proton forms one (value of p in the Fig. 1) hydrogen bond with a water molecule.

The interfacial structure with the evolution of charges and potential near the surface should be taken into account to properly reflect surface reactions. Several models have been proposed such as, for example, Triple Layer Model, Triple Plane Model or Basic Stern Model [34]. We chose to use the latter,

as proposed by Boily [35], due to its having fewer adjustable parameters. The value of the capacitance has been chosen at 0.92 F/m^2, in the range of the typical values found for modelling metal (hydr)oxides.

3. RESULTS AND DISCUSSION

3.1 Description of surface from DFT calculations

Table 1 and figure 2 present, for the main orientations of γ-Al_2O_3, the different sort of OH groups present in the surface models of Digne and co-workers at the highest water coverage considered in reference [13] (0.17 and 0.18 OH/nm^2 for the (100) and (110) orientations, respectively) and used in the Ab Initio Molecular Dynamics study of Ngouana-Wakou *et al.* [9] . Chemisorbed water molecules are referred to as H_2O sites; OH groups are referred to as μ_n sites, where n stands for the number of aluminum atoms bonded to the central oxygen atom. Transition aluminas contain two different types of aluminum atoms: six-coordinated and four-coordinated atoms in octahedral (Al_{VI}) and tetrahedral (Al_{IV}) environments, respectively. The nature of the Al involved in the different OH groups are listed in column 2 of Table 1 and illustrated in Fig. 2.

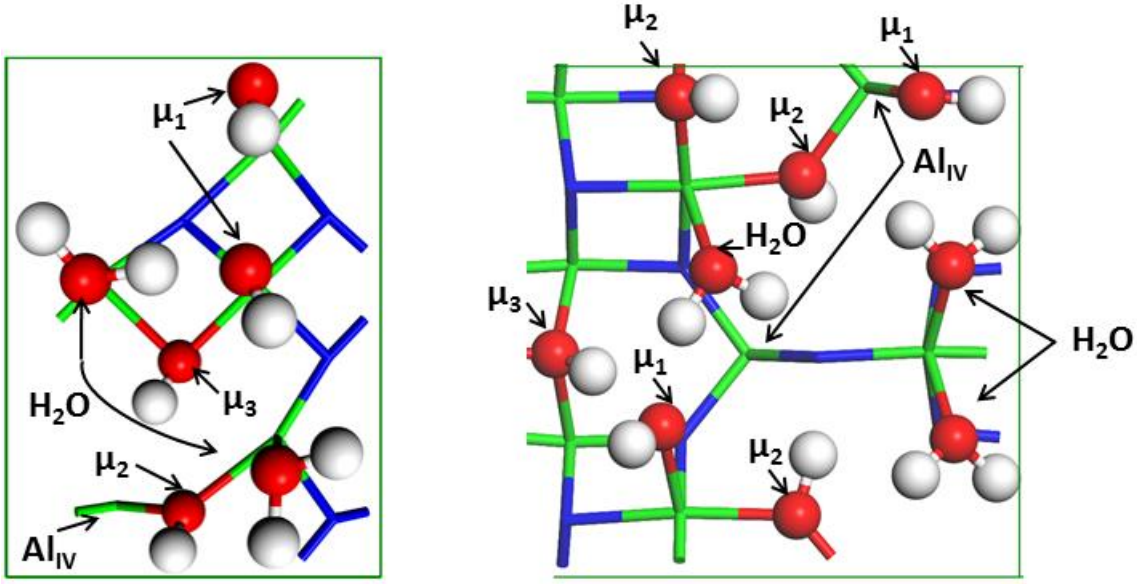

Fig. 2: From left to right, (1x1) representation of the (100) and (110) γ-Al_2O_3 surface orientations considered in this work (only the uppermost atoms are shown). Aluminum atoms are shown in green, hydrogen atoms in white and oxygen in surface and OH groups are shown in blue and red, respectively. Al atoms are in VI coordination unless otherwise stated.

Table 1. Characteristics of γ-Al_2O_3 surface OH groups from references [9,20] at water coverages of 0.17 and 0.18 OH/nm^2 for the (100) and (110) orientations, respectively (see figure 2)

OH site	Al involved	Amount in simulation box*		Surface Density (nm^{-2})	
		(100)	(110)	(100)	(110)
H_2O	Al_{VI}	2	3	4.31	4.48
μ_1	Al_{VI}	2	1	4.31	1.49
μ_1	Al_{IV}	0	1	0	1.49
μ_2	Al_{VI} and Al_{IV}	1	2	2.16	2.98
μ_2	Only Al_{VI}	0	1	0	1.49
μ_3	Only Al_{VI}	1	1	2.16	1.49

* unit cell vectors (u,v) for the (100) surface: 8.36 and 5.55 Å; for the (110) surface: 8.03 and 8.36 Å.

3.2 Calculation of protonation constants

Protonation constants were calculated for each site using the MUSIC model from Hiemstra et al. [15,16] with corrections accounting for the influence of hydrogen bonds at the solid-liquid interface based on the bond-valence principle in reference [18]. For the latter, we considered two approaches: firstly, by choosing to set the number of hydrogen bonds around the oxygen atom of the hydroxyl group arbitrarily to the one in ice (as in reference [18]); secondly, by using for Al_nOH surface species at the Point of Zero Charge the average number of hydrogen bonds obtained from AIMD simulations in reference [9]. The results of both approaches are presented in tables 2 and 3, respectively.

Table 2. Calculation of protonation constants using the number of H bonds around oxygen atoms in hydroxyl groups (a+d) as defined in [16].

OH	Al involved	Protonation reaction	Log K	Number of H bonds

site				with oxygen atom
μ_1	Al_{IV}	$\mu_1OH^{-0.25} + H^+ \leftrightarrows \mu_1OH_2^{0.75}$	4.95	2
μ_1	Al_{VI}	$\mu_1OH^{-0.5} + H^+ \leftrightarrows \mu_1OH_2^{0.5}$	9.9	2
μ_2	Al_{VI} and Al_{IV}	$\mu_2O^{-0.75} + H^+ \leftrightarrows \mu_2OH^{0.25}$	6.93	2
μ_2	Only Al_{VI}	$\mu_2O^{-} + H^+ \leftrightarrows \mu_2OH$	11.88	2
μ_3	Only Al_{VI}	$\mu_3O^{-0.5} + H^+ \leftrightarrows \mu_3OH^{0.5}$	5.94	1

Table 3. Calculation of protonation constants using a number of H bonds around oxygen atoms in hydroxyl groups (a+d) obtained from AIMD simulations in [9].

OH site	Al involved	Protonation reaction	Log K	Number of H bonds with oxygen atom
		Surface (100)		
μ_1	Al_{VI}	$\mu_1OH^{-0.5} + H^+ \leftrightarrows \mu_1OH_2^{0.5}$	8.72	2.3
μ_2	Al_{VI}-Al_{IV}	$\mu_2O^{-0.75} + H^+ \leftrightarrows \mu_2OH^{0.25}$	10.32	1.15
μ_3	Al_{VI}	$\mu_3O^{-0.5} + H^+ \leftrightarrows \mu_3OH^{0.5}$	5.94	1
		Surface (110)		
μ_1	Al_{IV}	$\mu_1OH^{-0.25} + H^+ \leftrightarrows \mu_1OH_2^{0.75}$	1.09	3
μ_1	Al_{IV}	$\mu_1O^{-1.25} + H^+ \leftrightarrows \mu_1OH^{-0.25}$	12.97	3
μ_1	Al_{VI}	$\mu_1OH^{-0.5} + H^+ \leftrightarrows \mu_1OH_2^{0.5}$	9.34	2.1
μ_2	Al_{VI}-Al_{IV}	$\mu_2O^{-0.75} + H^+ \leftrightarrows \mu_2OH^{0.25}$	10.45	1.1
μ_2	Al_{VI}-Al_{VI}	$\mu_2OH^0 + H^+ \leftrightarrows \mu_2OH_2^{+1}$	1.98	1.5
μ_2	Al_{VI}-Al_{VI}	$\mu_2O^{-1} + H^+ \leftrightarrows \mu_2OH^0$	13.86	1.5
μ_3	Al_{VI}	$\mu_3O^{-0.5} + H^+ \leftrightarrows \mu_3OH^{0.5}$	4.75	1.3

The deprotonated surface group with a (negative) charge z, Al_nO^z, can react twice with one proton, allowing the calculation of two successive protonation constants. The difference between some of these constants are more than 10 log units, and only those in the pH range 0-14 are listed in the Table 2.

The protonation constants of surface groups involving Al atoms of octahedral geometry are similar to those calculated on gibbsite surfaces in [36]; surface sites involving Al atoms in tetrahedral positions are more acidic, since there is a stronger Al to O charge transfer in O bonded to Al_{IV} sites (charge 3/4) than to Al_{VI} sites (charge 3/6).

Using the number of water molecules obtained by AIMD simulation in ref. [9], the undersaturation of the oxygen atoms can be refined. For instance, sites with the same local structure μ_n become

different for each face, since DFT simulations have shown that the structure of the water molecule in interaction with the surface depends on the orientation of the face (see [9]).

The values of protonation constants illustrate the strong effect of the number of hydrogen bonds. Thus, for $\mu_1(Al_{IV})$ on the (110) surface, compared to the ice structure, one more hydrogen bond has been found. This leads to a decrease of the second protonation constant of about 4 log unit, and allows to the first protonation to occur below pH 14. An opposite effect is seen for $\mu_2(Al_{VI}\text{-}Al_{VI})$, with a lower mean number of hydrogen bonds (between 1 and 1.5 instead of 2), and an increase of log K for the two protonations.

In the calculation of pKas, another assumption is made concerning the charge of the proton of the hydroxyl group, in interaction with surrounding water molecules by hydrogen bonds. In the initial model, one $Al_nOH\ldots OH_2$ bond is formed for each proton of surface OH groups. The charge +1 of the proton decreased to +0.8 due to the formation of one H donating bond. However, this choice for the number of hydrogen bonds comes from an analogy with ideal bulk water, and the real number of H donating bonds could be different. AIMD calculations allow to determine the mean number of water molecules involved in H donating bonds and can be used instead of the arbitrarily set value of 1 (p in Figure 1). This value is important because it has an impact on the second protonation constant since the calculation of this value is based on the geometry of the surface group after the first protonation step.

In Table 4 it can be seen that the arbitrarily and generally used set value of 1 hydrogen bond is slightly overestimated. This can be explained by steric effects at the surface. Thus, instead of +0.8 units, the charge of H will increase following the relation 1-0.2p. However, these results show that a 25% decrease in the H charge leads to a small decrease of about 1 log unit for K.

Table 4. Calculation of protonation constants using AIMD simulations to determine the number of H bonds around oxygen atoms in hydroxyl groups (a+d), and the number of H bonds around their respective protons (p).

OH site	Al involved	Protonation reaction	Log K	Number of H bonds with proton*
		Surface (100)		
μ_1	Al_{VI}	$\mu_1OH^{-0.5} + H^+ \leftrightarrows \mu_1OH_2^{0.5}$	8.16	0.86
μ_2	Al_{VI}-Al_{IV}	$\mu_2O^{-0.75} + H^+ \leftrightarrows \mu_2OH^{0.25}$	10.32	n.a.
μ_3	Al_{VI}	$\mu_3O^{-0.5} + H^+ \leftrightarrows \mu_3OH^{0.5}$	5.94	n.a.
		Surface (110)		
μ_1	Al_{IV}	$\mu_1OH^{-0.25} + H^+ \leftrightarrows \mu_1OH_2^{0.75}$	0.12	0.75
μ_1	Al_{IV}	$\mu_1O^{-1.25} + H^+ \leftrightarrows \mu_1OH^{-0.25}$	12.97	n.a.
μ_1	Al_{VI}	$\mu_1OH^{-0.5} + H^+ \leftrightarrows \mu_1OH_2^{0.5}$	9.16	0.95
μ_2	Al_{VI}-Al_{IV}	$\mu_2O^{-0.75} + H^+ \leftrightarrows \mu_2OH^{0.25}$	10.45	n.a.
μ_2	Al_{VI}-Al_{VI}	$\mu_2OH^{0.25} + H^+ \leftrightarrows \mu_2OH_2^{1.25}$	0.29	0.57
μ_2	Al_{VI}-Al_{VI}	$\mu_2O^{-0.75} + H^+ \leftrightarrows \mu_2OH^{0.25}$	13.86	n.a.
μ_3	Al_{VI}	$\mu_3O^{-0.5} + H^+ \leftrightarrows \mu_3OH^{0.5}$	4.75	n.a.

* for H bonds around oxygen, see Table 3. n.a.: non applicable since the site is deprotonated.

One of the surface sites obtained by DFT simulations (Table 1, first line), consists on a surface aluminum atom with a chemisorbed water molecule. We consider μ_1-H_2O groups as interfacial water molecules and thus neglect them in the chemical equations considered in the interfacial model. Indeed, if we assume that the interaction of H_2O molecules with the support is weak and therefore the pKa of these molecules is the same as those in bulk water. The model described above (Table 4) has been implemented in PHREEQC and the curves of surface charge have been simulated for three different ionic strengths (Fig. 3). The result follows the general trends found in aluminum (hydr)oxides titration curves with a PZC around 8-9 [37].

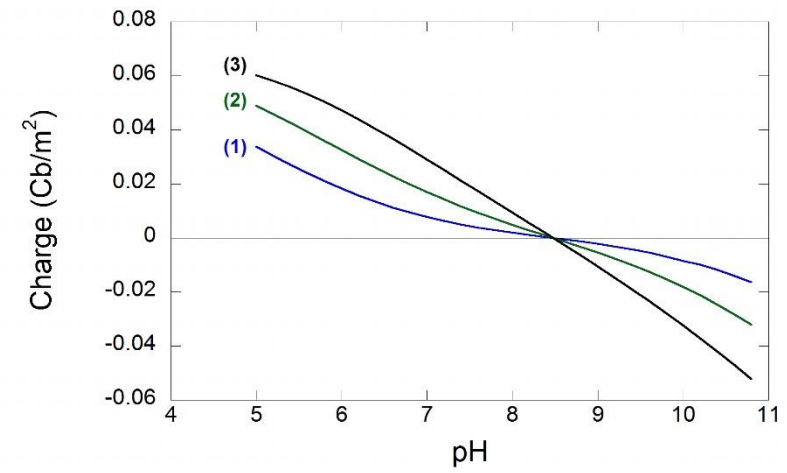

Fig.3. Simulated surface charge curves at different ionic strengths from the DFT-MUSIC model (protonation constants in Table 4): (1) 1 mM, (2) 10 mM and (3) 100 mM.

The surface speciation is then detailed for a given ionic strength (1 mM). The protonation fraction of each site for both faces as a function of pH is shown in Fig. 4. Several groups neither release nor accept H from interfacial water. Therefore, for both faces, fluctuations in surface charge can be accounted for by the interaction of $\mu_{1,VI}$-OH with interfacial water. Besides, and in accordance with the analysis in reference [9], the interaction of these sites with the solvent is stronger in the (110) orientation.

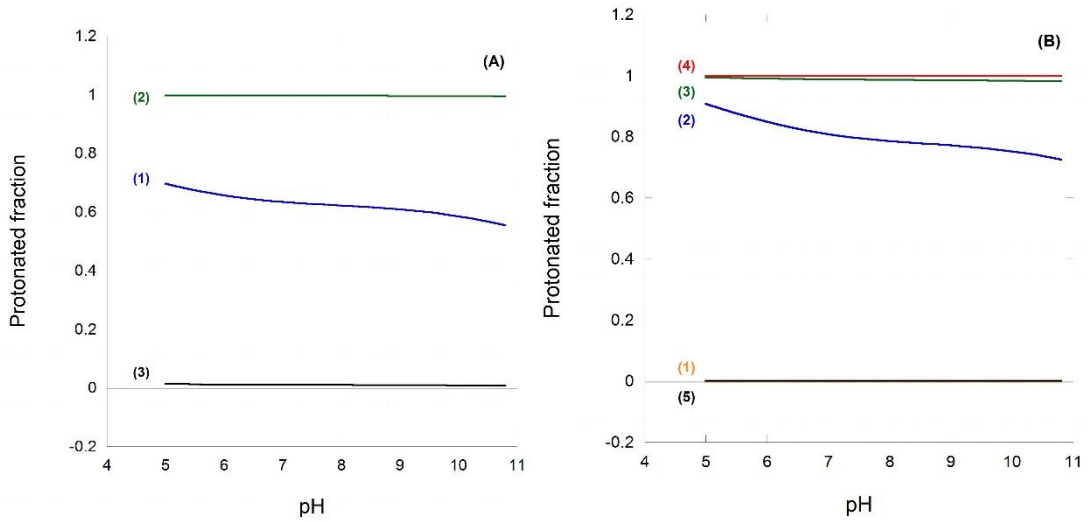

Fig. 4. Protonated fraction of each sites as a function of pH from calculation by the DFT-MUSIC model without μ_1-H_2O sites: (A) face (100) for (1) μ_1-Al_{VI} (diprotonated/mono-), (2) μ_2-Al_{VI}-Al_{IV} (mono-/de-) and (3) μ_3-Al_{VI} (mono-/de-) and (B) face (110) for (1) μ_1-Al_{IV} (di-/mono-) (2) μ_1-Al_{VI} (di-/mono-), (3) μ_2-Al_{VI}-Al_{IV} (mono-/de-), (4) μ_2-Al_{VI}-Al_{VI} (mono-/de-) and (5) μ_3-Al_{VI} (mono-/de-). The indicated acid/base couple (mono- or di- / de- or mono-) correspond to the equilibria detailed in Table 3.

Moreover, at all pH values considered in this work, μ_3-OH groups lose their proton readily. This is an interesting result since there is evidence that μ_3-OH are present at the solid-gas interface [13]. Hence, μ_3 may tend to capture protons from liquid water during the drying process of alumina. This is a demonstration that the reactivity of a surface sites depends on the surrounding media and therefore, in order to rationalize adsorption processes at the solid liquid interface, materials characterizations need to be done in the presence of the encompassing liquid phase.

The simulated curves have been compared to experimental titrations carried out on γ-alumina (Fig. 7). The detailed outcomes for experimental surface charge are described in reference [22].

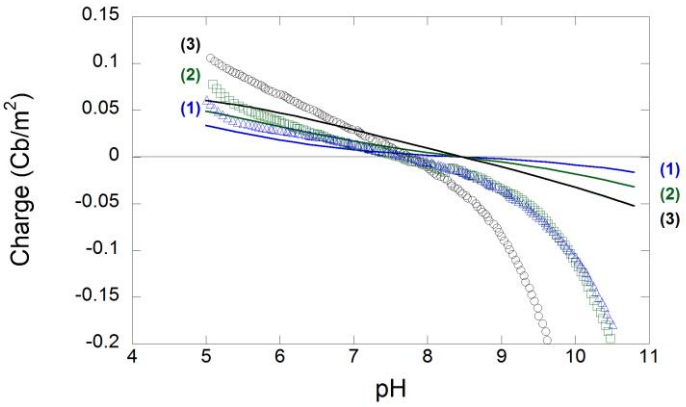

Fig. 7. Surface charge curves at different ionic strengths (1) 1 mM, (2) 10 mM and (3) 100 mM from experiments (dots) and simulations (line).

Keeping in mind that the simulated curves are not based on any fitting parameters, they can be considered as in good qualitative agreement with experiment at pH below 9. Moreover, effects induced by the ionic strength are well reproduced and PZC are in reasonable good agreement with experiments. Beyond the pH value of 9, the match between the experimental and theoretical curves worsens, due to the asymmetry of the experimental titration curves, whose slopes are higher above pzc, as this has been previously observed by Hiemstra et al. This trend cannot be captured by a model based only on protonation surface reactions, which give intrinsically concentration evolutions symmetrical on both sides of pKa. To solve this problem, authors have used the possibility to form surface ion pairs between charged surface hydroxyls and electrolyte ions according to the following general equations, where A^- and C^+ are respectively inert anion (Cl^-, NO_3^-) or cation (Na^+, K^+), respectively.

$Al_nOH_d^{z+d} + A^- \leftrightarrows Al_nOH_dA^{z+d-1}$ $K_{c,A}$ with z+d > 0 (2)

$Al_nOH_d^{z+d} + C^+ \leftrightarrows Al_nOH_dC^{z+d+1}$ $K_{c,C}$ with z+d < 0 (3)

The formation of surface ion pairs decreased the surface potential, in absolute value, and so the electrostatic repulsion between surface and H^+/OH^- ions. It allows to increase the surface density of (de)protonated groups.

The direct measurement of the constants remains difficult, and they are generally obtained from the fitting of acid-base curves and a difference in the behavior of cations and anions can be at the origin of the asymmetry. Thus, Hiemstra et al. have suggested that Cl^- are able to reach subsurface hydroxyl sites, modifying the impact of counter-ions on the surface concentration of positive or negative groups. Mayordomo et al. [20] have used a more common approach, with a higher value for $K_{c,Na}$ (0.8 vs. 0.67 for $K_{c,Cl}$). In a first attempt to take into account surface ion pairs in the modelling, the same simulation has been done including the equilibria (2) and (3) for all the charged surface species. Values from Mayordomo et al. [20] have been used for adsorption of cations or anions, along with the electrostatic model they used (TLM). The result is shown in Fig. 8. As expected, two effects can be seen: a global increase of the surface charge (in absolute value), stronger in the pH range where surface is negative.

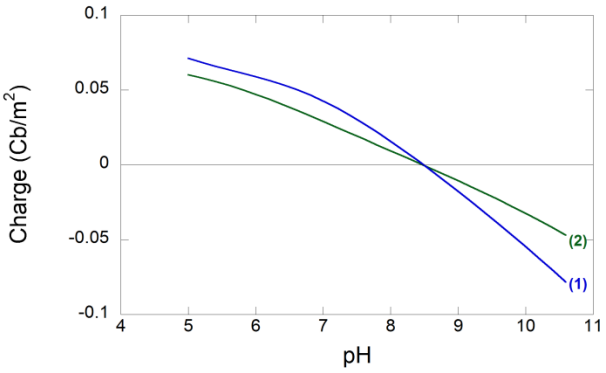

Fig. 8. Simulated surface charge curves at an ionic strength of 100 mM using DFT-MUSIC model (1) with and (2) without surface ion pairs formation.

This calculation illustrates the importance of surface ion pair formation in the prediction of surface charging. The current approach is rather rough, due to the lack of independent data on adsorption of counter-ions. The modelling of these reactions would be an important step in the understanding of the interface structure.

4. CONCLUSIONS

The different simulations presented in this work show to what extent atomic scale structural data – obtained from Density Functional Theory calculations- can be used with the MUSIC model to simulate the speciation in solution of surface sites on the poorly crystalline material, γ-Al_2O_3. The results presented are in qualitative agreement with experimental data, despite the absence of any fitting parameter. Hence, although more elaborate theoretical calculations need to be performed in order to get a better match between simulation and experiment, the atomistic model for γ-Al_2O_3 surfaces from Digne and co-workers [13] can be used with the methodology presented herein to obtain the speciation of this material in suspension at the initial stages of the impregnation or chemical weathering of γ-Al_2O_3 and seems an appropriate starting point to improve MUSIC based results with more demanding theoretical calculations in the future as the ones done in [38] at the DFT level.

According to our simulations, the pH of interfacial water seems to affect mostly the speciation of alumina $\mu_{1,VI}$-OH groups. These results could be used for the interpretation of complexation data or a refinement of a heterogeneous catalyst preparation by an impregnation technique. Moreover, future and more complex AIMD simulations for the description of the chemical weathering phenomena of

this material (as in [10]) could benefit from this result allowing researchers to focus on the most reactive sites of this complex system.

ACKNOWLEDGMENTS

We would like to acknowledge Dr. P. Raybaud (IFP Energies nouvelles) is also greatly acknowledged for fruitful discussions and a review of an initial version of this manuscript. This work was supported by the French National Research Agency within the framework of the ANR-14-CE08-0019 SLIMCAT project. Calculations were performed using HPC resources from GENCI-CINES (Grant A0020807386).

References

(1) Euzen, P.; Raybaud, P.; Krokidis, X.; Toulhoat, H.; Le Loarer, J.; Le Loarer, J. L.; Froidefond, C. Alumina. In *Handbook of Porous Solids*; Schüth, F., Sing, K. S. W., Weitkamp, J., Eds.; Wiley-VCH Verlag GmbH: Weinheim, 2002, pp. 1591–1677.

(2) Kasprzyk-Hordern, B. Chemistry of Alumina, Reactions in Aqueous Solution and its Application in Water Treatment. *Adv. Colloid Interface Sci.* **2004**, *110* (1-2), 19–48.

(3) Raybaud, P.; Chizallet, C.; Mager-Maury, C.; Digne, M.; Toulhoat, H.; Sautet, P. From γ-Alumina to Supported Platinum Nanoclusters in Reforming Conditions: 10 Years of DFT Modeling and Beyond. *J. Catal.* **2013**, *308*, 328–340.

(4) Raybaud, P.; Costa, D.; Valero, M. C.; Arrouvel, C.; Digne, M.; Sautet, P.; Toulhoat, H. First Principles Surface Thermodynamics of Industrial Supported Catalysts in Working Conditions. *J. Phys. Condens. Matter* **2008**, *20* (6), 64235.

(5) Abi Aad, J.; Casale, S.; Michau, M.; Courty, P.; Diehl, F.; Marceau, E.; Carrier, X. Chemical Weathering of Alumina in Aqueous Suspension at Ambient Pressure: A Mechanistic Study. *ChemCatChem* **2017**, *9* (12), 2186–2194.

(6) Lefèvre, G.; Duc, M.; Lepeut, P.; Caplain, R.; Fédoroff, M. Hydration of γ-Alumina in Water and Its Effects on Surface Reactivity. *Langmuir* **2002**, *18* (20), 7530–7537.

(7) Abi Aad, J.; Courty, P.; Decottignies, D.; Michau, M.; Diehl, F.; Carrier, X.; Marceau, E. Inhibition by Inorganic Dopants of γ-Alumina Chemical Weathering Under Hydrothermal Conditions: Identification of Reactive Sites and their Influence in Fischer-Tropsch Synthesis. *ChemCatChem* **2017**, *9* (12), 2106–2117.

(8) Réocreux, R.; Jiang, T.; Iannuzzi, M.; Michel, C.; Sautet, P. Structuration and Dynamics of Interfacial Liquid Water at Hydrated γ-Alumina Determined by ab Initio Molecular Simulations: Implications for Nanoparticle Stability. *ACS Appl. Nano Mater.* **2018**, *1* (1), 191–199.

(9) Ngouana-Wakou, B. F.; Cornette, P.; Corral Valero, M.; Costa, D.; Raybaud, P. An Atomistic Description of the γ-Alumina/Water Interface Revealed by Ab Initio Molecular Dynamics. *J. Phys. Chem. C* **2017**, *121* (19), 10351–10363.

(10) Romain Réocreux. *Biomass Derivatives in Heterogeneous Catalysis: Adsorption, Reactivity and Support from First Principles*. PhD: ENS-Lyon, 2017.

(11) Bourikas, K.; Kordulis, C.; Lycourghiotis, A. The Mechanism of the Protonation of Metal (Hydr)Oxides in Aqueous Solutions Studied for Various Interfacial/Surface Ionization Models and Physicochemical Parameters: a Critical Review and a Novel Approach. *Adv. Colloid Interface Sci.* **2006**, *121* (1-3), 111–130.

(12) Kummert, R.; Stumm, W. The Surface Complexation of Organic Acids on Hydrous γ-Al_2O_3. *J. Colloid Interface Sci.* **1980**, *75* (2), 373–385.

(13) Digne, M.; Sautet, P.; Raybaud, P.; Euzen, P.; Toulhoat, H. Hydroxyl Groups on Gamma-Alumina Surfaces: A DFT Study. *J. Catal.* **2002**, *211*, 1–5.

(14) Digne, M.; Sautet, P.; Raybaud, P.; Euzen, P.; Toulhoat, H. Use of DFT to Achieve a Rational Understanding of Acid-Basic Properties of Gamma-Alumina Surfaces. *J. Catal.* **2004**, *226*, 54–68.

(15) Hiemstra, T.; De Wit, J. C. M.; Van Riemsdijk, W. H. Multisite Proton Adsorption Modeling at the Solid/Solution Interface of (Hydr)Oxides: A New Approach: II. Application to Various Important (Hydr)Oxides. *J. Colloid Interface Sci.* **1989**, *133* (1), 105–117.

(16) Hiemstra, T.; Van Riemsdijk, W. H.; Bolt, G. H. Multisite Proton Adsorption Modeling at the Solid/Solution Interface of (Hydr)Oxides: A New Approach: I. Model Description and Evaluation of Intrinsic Reaction Constants. *J. Colloid Interface Sci.* **1989**, *133* (1), 91–104.
(17) Hiemstra, T.; Van Riemsdijk, W. H. A Surface Structural Approach to Ion Adsorption: The Charge Distribution (CD) Model. *J. Colloid Interface Sci.* **1996**, *179* (2), 488–508.
(18) Hiemstra, T.; Venema, P.; Riemsdijk, W. H. Van. Intrinsic Proton Affinity of Reactive Surface Groups of Metal (Hydr)oxides: The Bond Valence Principle. *J. Colloid Interface Sci.* **1996**, *184* (2), 680–692.
(19) Tang, C.; Giaume, D.; Guerlou-Demourgues, L.; Lefèvre, G.; Barboux, P. Prediction of Isoelectric Point of Manganese and Cobalt Lamellar Oxides: Application to Controlled Synthesis of Mixed Oxides. *Langmuir* **2018**, *34* (23), 6670–6677.
(20) Mayordomo, N.; Foerstendorf, H.; Lützenkirchen, J.; Heim, K.; Weiss, S.; Alonso, U.; Missana, T.; Schmeide, K.; Jordan, N. Selenium(IV) Sorption Onto γ-Al2O3: A Consistent Description of the Surface Speciation by Spectroscopy and Thermodynamic Modeling. *Environ. Sci. Technol.* **2018**, *52* (2), 581–588.
(21) Kazuomi Nagashima; Frank D Blum. Proton Adsorption onto Alumina: Extension of Multisite Complexation (MUSIC) Theory. *J. Colloid Interface Sci.* **1999**, *217* (1), 28–36.
(22) Machesky, M. L.; Predota, M.; Wesolowski, D. J.; Vlcek, L.; Cummings, P. T.; Rosenqvist, J.; Ridley, M. K.; Kubicki, J. D.; Bandura, A. V.; Kumar, N.; Sofo, J. O. Surface Protonation at the Rutile (110) Interface: Explicit Incorporation of Solvation Structure within the Refined MUSIC Model Framework. *Langmuir* **2008**, *24* (21), 12331–12339.
(23) Ridley, M. K.; Machesky, M. L.; Kubicki, J. D. Anatase Nanoparticle Surface Reactivity in NaCl Media: A CD-MUSIC Model Interpretation of Combined Experimental and Density Functional Theory Studies. *Langmuir* **2013**, *29* (27), 8572–8583.
(24) Parkhurst D. L., Appelo C. *User's guide to PHREEQC (version 2)— A computer program for speciation, batch-reaction, one-dimensional transport, and inverse geochemical calculations, Water-Resources Investigations USGS*, 1999.
(25) Ali Ahmad, M.; Zajac, J.; Prelot, B. Sorption Behavior of Co(II)-γ-alumina System in the Presence of Organic Additives. *J. Colloid Interface Sci.* **2019**, *535*, 182–194.
(26) Ali Ahmad, M.; Prelot, B.; Dufour, F.; Durupthy, O.; Razafitianamaharavo, A.; Douillard, J. M.; Chaneac, C.; Villiéras, F.; Zajac, J. Influence of Morphology and Crystallinity on Surface Reactivity of Nanosized Anatase TiO2 Studied by Adsorption Techniques. 2. Solid–Liquid Interface. *J. Phys. Chem. C* **2013**, *117* (9), 4459–4469.
(27) Krokidis, X.; Raybaud, P.; Gobichon, A. E.; Rebours, B.; Euzen, P.; Toulhoat, H. Theoretical Study of the Dehydration Process of Boehmite to gamma-Alumina. *J. Phys. Chem. B* **2001**, *105* (22), 5121–5130.
(28) Lippens, B. C.; Boer, J. H. de. Study of Phase Transformations During Calcination of Aluminum Hydroxides by Selected Area Electron Diffraction. *Acta Crystallogr.* **1964**, *17* (10), 1312–1321.
(29) VandeVondele, J.; Krack, M.; Mohamed, F.; Parrinello, M.; Chassaing, T.; Hutter, J. Quickstep: Fast and Accurate Density Functional Calculations Using a Mixed Gaussian and Plane Waves Approach. *Comput. Phys. Commun.* **2005**, *167* (2), 103–128.
(30) Perdew; Burke; Ernzerhof. Generalized Gradient Approximation Made Simple. *Phys. Rev. Lett.* **1996**, *77* (18), 3865–3868.
(31) Perdew, J. P.; Burke, K.; Ernzerhof, M. Generalized Gradient Approximation Made Simple [Phys. Rev. Lett. 77, 3865 (1996)]. *Phys. Rev. Lett.* **1997**, *78* (7), 1396.

(32) Grimme, S. Semiempirical GGA-Type Density Functional Constructed with a Long-Range Dispersion Correction. *J. Comput. Chem.* **2006**, *27* (15), 1787–1799.
(33) Goedecker, S.; Teter, M.; Hutter, J. Separable Dual-Space Gaussian Pseudopotentials. *Phys. Rev. B* **1996**, *54* (3), 1703–1710.
(34) Lützenkirchen, J. Surface Complexation Models of Adsorption. In *Encyclopedia of Surface and Colloid Science*, 3rd ed.; P. Somasundaran, Ed.; CRC Press: Boca Raton, 2015, pp. 5028–5046.
(35) Boily, J.-F.; Lützenkirchen, J.; Balmès, O.; Beattie, J.; Sjöberg, S. Modeling Proton Binding at the Goethite (α-FeOOH)–Water Interface. *Colloids Surf. A Physicochem. Eng. Asp.* **2001**, *179* (1), 11–27.
(36) Yong, H.; Van Riemsdijk, W. H. Interfacial Charging Phenomena of Aluminum (Hydr)oxides. *Langmuir* **1999**, *15* (18), 5942–5955.
(37) Kosmulski, M. Chemical Properties of Material Surfaces. In *Surfactant Science Series, vol. 102*; Hubbard, A. T., Ed.; Marcel Dekker, Inc.: New York, 2002; Vols. 102.
(38) Sulpizi, M.; Sprik, M. Acidity Constants from Vertical Energy Gaps: Density Functional Theory Based Molecular Dynamics Implementation. *Phys. Chem. Chem. Phys.* **2008**, *10* (34), 5238–5249.